Multispacecraft study on the dynamics of the dusk-flank magnetosphere under northward IMF: 10–11 January 1997

H. Stenuit,[1] M. Fujimoto,[2] S. A. Fuselier,[3] J.-A. Sauvaud,[1] S. Wing,[4] A. Fedorov,[1] E. Budnik,[1] S. P. Savin,[5] K. J. Trattner,[3] V. Angelopoulos,[6] J. Bonnell,[6] T. D. Phan,[6] T. Mukai,[7] and A. Pedersen[8]

Received 4 January 2002; revised 22 March 2002; accepted 27 March 2002; published 31 October 2002.

[1] The latter half of the magnetic cloud event on 10–11 January 1997 is studied in the context of the cold-dense plasma sheet. A fortuitous distribution of spacecraft in key regions allows us to relate the plasma sheet status transition with the boundary layer process. When the interplanetary magnetic field (IMF) was strongly northward and the solar wind density returned to a nominal value from an anomalously large one, two spacecraft, Geotail and Interball-Tail, were in the dusk-flank region and detected a change in the plasma sheet status from hot and tenuous to cold and dense. The change seen by these spacecraft making in situ observations is confirmed to be a global feature by DMSP observations at low altitude. Just around this time, Interball-Aurora and Polar were crossing the dusk-auroral oval, monitoring globally the dynamics of the dusk-flank magnetopause at its footpoint. Injection of magnetosheath-like ions was detected by these spacecraft. We try to relate these observations with the processes that transport the magnetosheath plasma onto the magnetospheric field lines. Three candidate processes are discussed, but none of them turn out to be convincing, indicating the need for further study on this issue. *INDEX TERMS:* 2764 Magnetospheric Physics: Plasma sheet; 2784 Magnetospheric Physics: Solar wind/magnetosphere interactions; 2724 Magnetospheric Physics: Magnetopause, cusp, and boundary layers; *KEYWORDS:* magnetosphere, dusk flank, northward interplanetary magnetic field, auroral regions, boundary layer

Citation: Stenuit, H., et al., Multispacecraft study on the dynamics of the dusk-flank magnetosphere under northward IMF: 10–11 January 1997, *J. Geophys. Res.*, *107*(A10), 1333, doi:10.1029/2002JA009246, 2002.

1. Introduction

[2] A magnetic cloud produced by a coronal mass ejection event hit the Earth's magnetosphere on 10–11 January 1997. The former half of the cloud had strong southward magnetic field component and caused a severe magnetic storm, which has been studied extensively (see, for example, papers in the special issue of *Geophysical Research Letters*, vol. 25(14), 1998). The latter half of the interval with strong northward interplanetary magnetic field (IMF) has been studied by several authors [e.g., *Sandahl et al.*, 1998; *Farrugia et al.*, 2000]. We will also study this interval, focusing on the dynamics of dusk flank. We try to relate this region with the concurrent change in the plasma sheet status from hot-tenuous to cold-dense. Such a change is characteristic of northward IMF intervals.

[3] The plasma sheet is now well-known to become cold and dense ($n \sim 1$ cm^{-3}, $T \sim 1$ keV) during northward IMF periods [e.g., *Terasawa et al.*, 1997]. Studies on this issue show that the presence of the magnetosheath-like ions are responsible for this cold-dense status [*Fuselier et al.*, 1999] that is totally different from southward IMF periods. The magnetosheath-like ions are only weakly heated and are occasionally distinctly separated from the several keV plasma sheet components. This results in a two-component feature in an Et diagram [e.g., *Fujimoto et al.*, 1998]. That is, the cold magnetosheath component and the plasma sheet component can be mixed spatially with relatively little mixing in energy. The mixed ions, whose appearance is quite similar to the ions in the dayside inner boundary layer [*Le et al.*, 1996], have been observed more frequently in the dusk-flank plasma sheet during periods of persistent northward IMF [*Fujimoto et al.*, 1998; *Fuselier et al.*, 1999; *Phan et al.*, 2000]. Similarly magnetosheath-like electrons and mixed plasma sheet and magnetosheath are more frequently observed inside the magnetospheric flanks during northward IMF [e.g., *Mitchell et al.*, 1987; *Sauvaud et al.*, 1997]. While some ideas have been proposed to explain how plasmas from two different sources come to coexist on the same magnetospheric field lines [e.g,, *Lennartsson*,

[1]Centre d'Etude Spatiale des Rayonnements, CNRS, Toulouse, France.
[2]Department of Earth and Planetary Science, Tokyo Institute of Technology, Tokyo, Japan.
[3]Lockheed Martin Palo Alto Laboratory, Palo Alto, California, USA.
[4]Applied Physics Laboratory, Johns Hopkins University, Laurel, Maryland, USA.
[5]Space Research Institute, Academy of Sciences, Moscow, Russia.
[6]Space Sciences Laboratory, Berkeley, California, USA.
[7]Institute of Space and Astronautical Science, Sagamihara, Japan.
[8]Department of Physics, Oslo University, Oslo, Norway.

0148-0227/02/2002JA009246$09.00

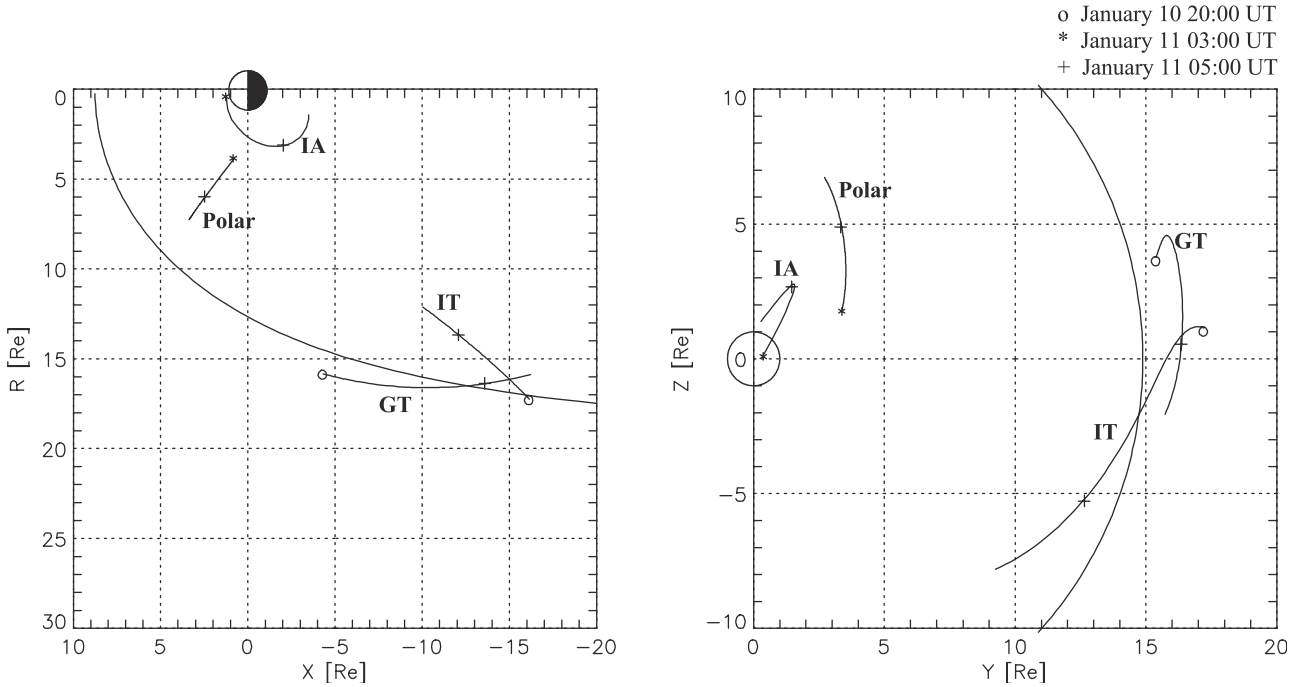

Figure 1. Orbits of Geotail and Interball-Tail between 10 January 1997, 2000 UT, and 11 January 1997, 0800 UT, and Polar and Interball-Auroral between 11 January 1997, 0300 UT and 0700 UT in the *XR* and *YZ* GSM plane. The magnetopause shape is computed from the *Shue et al.* [1998] model for an average dynamic pressure over the considered period. In the *YZ* GSM plane, the magnetopause is represented at $X_{GSM} = -5\ R_E$. The "o", the "*" and the "+" symbols are located respectively at 2000 UT (10 January), 0300 UT (11 January) and 0500 UT (11 January).

1992; *Raeder et al.*, 1997; *White et al.*, 1998; *Nishikawa*, 1998; *Fuselier et al.*, 1999; *Fairfield et al.*, 2000; *Song et al.*, 2000], observations are still too limited to pin down the actual mixing process.

[4] The latter half of the magnetic cloud event on 10–11 January is used in this paper to study the formation of the cold-dense plasma sheet. This particular interval is well suited for this study not only because of the prolonged northward IMF interval but also because of the fortuitous distribution of spacecraft in the key regions of the magnetosphere. Figure 1 represents the orbits of Geotail and Interball-Tail between 10 January 1997, 2000 UT, and 11 January 1997, 0800 UT, and those of Polar and Interball-Auroral between 11 January 1997, 0300 UT and 0700 UT in the *XR* and *YZ* GSM plane. The magnetopause shape is computed from the *Shue et al.* [1998] model. The dynamic pressure averaged over the entire period of interest (~6 nPa) is used as an input parameter to the model. In the plot corresponding to the *YZ* plane, the magnetopause location at $X_{GSM} = -5\ R_E$ is also included. Our focus here is on the dusk–flank magnetopause and the plasma sheet. When the IMF was northward, two spacecraft, Geotail and Interball-Tail, were in the dusk-flank region. The change in characteristics of the plasma sheet seen in situ by these spacecraft is confirmed to be a global feature by DMSP observations at low altitude. Just around the time when the plasma sheet status was changing (0500 UT, 11 January), Interball-Aurora and Polar were crossing the dusk-auroral oval monitoring globally the dynamics of the dusk-flank magnetopause. Injection of magnetosheath-like ions was detected by both spacecraft. The solar wind density and thus the dynamic pressure varied considerably during this interval on 10–11 January. This variability results in complications in the interpretation, and possibly some difficulties in generalizing the observations to usual northward IMF periods. However, since both a cold and dense plasma sheet and recurrent auroral ion injections related to the magnetospheric flank are detected frequently during northward IMF [*Fujimoto et al.*, 1998; *Stenuit et al.*, 2001], this event allows us to learn more about the cold-dense plasma sheet and its relationship to injections, observed at lower altitudes.

2. Wind Observations of SW/IMF

[5] Figure 2 displays the velocity, the dynamic pressure of the solar wind and B_x, B_y and B_z components of IMF in Geocentric Solar Magnetospheric System (GSM) coordinates measured by Wind at (X_{gsm}, Y_{gsm}, Z_{gsm}) ~ (95, −56, −13) R_E between 10 January 1997, 1200 UT, and 11 January 1997, 1200 UT. A time delay of about 22 min should be applied to compare these data with measurements obtained for X ~ 0 R_E. Wind plasma and magnetic field data used in this study are from the SWE and MFI instruments, respectively, as described by *Ogilvie et al.* [1995] and *Lepping et al.* [1995]. The time resolution is 46 s. Since *Sandahl et al.* [1998] and *Farrugia et al.* [2000] have already described the Wind data in detail for this day, here, we will only point out the features that are of significant relevance for our work. The IMF B_z component turned positive at 2100 UT and the field stayed northward during most of the subsequent 12 hours. This condition is similar to the one described by *Fujimoto et al.* [2000], in which mixed

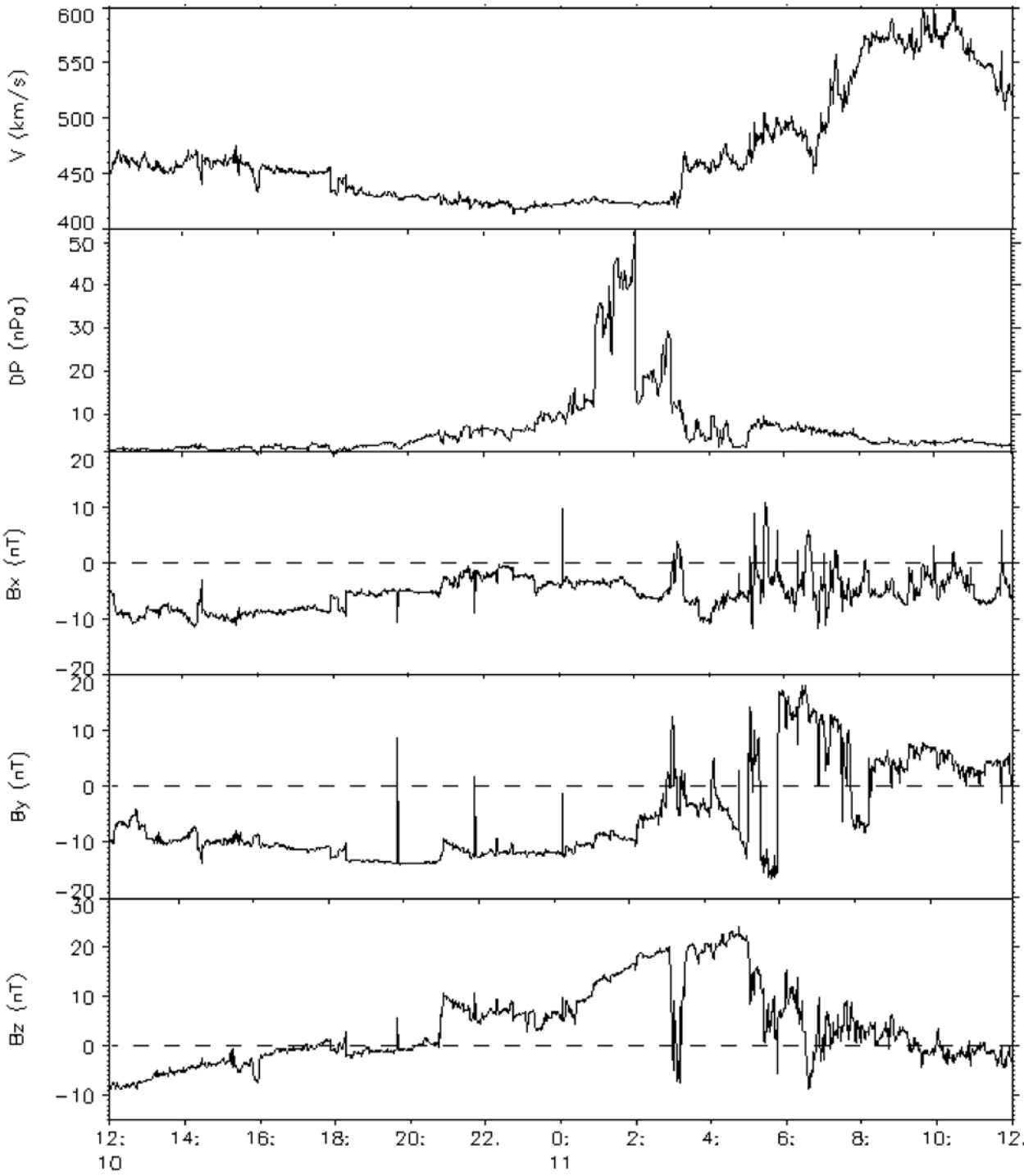

Figure 2. From top to bottom: Velocity (km s^{-1}), dynamic pressure (nPa) of the solar wind and B_x, B_y, B_z components in GSM coordinates of the interplanetary magnetic field measured by Wind from 10 January 1997, 1200 UT, to 11 January, 1200 UT.

ions are then detected close to the central axis of the magnetotail after 12 hours of northward IMF B_z. Around 2000 UT, the solar wind dynamic pressure started to increase gradually, due to the gradual increase in the solar wind density. There occurred a jump in the density and thus in the dynamic pressure from 10 to 35 nPa in less than 10 min around 0100 UT. This anomalously elevated dynamic pressure decreases around 0200 UT and again around 0300 UT. After the second decrease, the solar wind condition is more or less nominal. The IMF B_y and B_z components varied so that the interval 0130–0530 UT is characterized by a strongly northward feature $B_z > |B_y|$. The two-hour

interval between 0400 and 0600 UT is the key interval for our study. There are variations in the IMF B_y component, but as an overview the interval is characterized by strongly northward IMF and nominal solar wind conditions.

3. High-Altitude Observations

3.1. Geotail Observations

[6] The Geotail spacecraft (GT) was in the duskside plasma sheet (PS) when the solar wind density started to increase. The gradual increase in the solar wind dynamic pressure pushed the magnetopause (MP) in and brought GT into the boundary layer (BL) region at 2100 UT (10 January), at which time IMF had already turned northward. IMF stays mostly northward throughout the interval of interest described in this section. The data in Figure 3 shows that GT made numerous MP crossings from 2100–2400 UT while moving from (X_{gsm}, Y_{gsm}) = (−5.5, 15.6) to (−8.7, 16.0) R_E. This is most evident in the density (6th panel) and the ion temperature (7th panel) panels, in which excursions between hot-tenuous (>2 keV, <0.5 cm^{-3}) and cold-dense (<0.3 keV, >5 cm^{-3}) plasma are evident. The V_x component (2nd panel) also shows excursion between tailward flowing (−200 km/s) and mostly stagnant plasma and these switchings are accompanied by variations in the V_y component. The magnetic field data (B_x component, 1st panel) shows that the spacecraft was located at low latitude (small $|B_x|$) in the PS and the B_x component is strongly negative in the magnetosheath adjacent to MP. The negative B_x in the dusk-sheath region is not consistent with the normal draping of the field lines that had negative B_y in the upstream solar wind. Since B_z is positive in the sheath region (not shown), the field lines connect GT to a northern high-latitude part located further tailward. Judging from the GT location of Z_{gsm} = 4.2–4.5 R_E and slightly positive B_x in PS, the spacecraft was situated north of the equator. With these, the behavior of the magnetic field components can be understood in terms of the reversed draping, in which the tailward flowing field lines are most lagged behind close to the equator (south of the GT position) and are fastest at high latitudes. The vortex-like activity described below may have caused this equatorial lagging.

[7] In order to look into the nature of this flow variation, we have calculated 10 min averaged flow vectors ($\mathbf{V_{ave}}$) for every data point and subtracted them from the data to obtain the fluctuating component $\mathbf{dV} = \mathbf{V} - \mathbf{V_{ave}}$ in the *XY* GSM plane. The red traces in the 2nd and the 3rd panels in Figure 3 show the 10 min average flows and the 4th panel shows the amplitude of the fluctuating component. One can see that the flow characteristics in this BL region can be summarized as (V_x, V_y) = (−100 ± 100, 50 ± 50) km s^{-1}. Then the angle of the fluctuating component vector **dV** from the tailward direction (GSM-*X*) is computed. The duskward direction is defined to be π/2 (90°). For each complete rotation of the fluctuating component, 2π is added or subtracted to the data (depending of the clockwise or anticlockwise direction of the rotation of the fluctuating component). The variable *a*, shown in the 5th panel, is the angle of the fluctuating component vector **dV** from the tailward direction (GSM-*X*) divided by 2π. It corresponds to the number of vortices observed during the considered period and shows the rotating feature of the fluctuating component. Since *a* is mostly linearly increasing with time, the fluctuating component is showing a clockwise steady rotation. The angular frequency is calculated to be 3.3 mHz (that is, a 5 min period).

[8] From this analysis, we suggest that a sequence of tailward propagating vortices was present at the MP during this time interval. Figure 4 shows the idea schematically. Since the vortices are propagating tailward, the spacecraft (GT), nearly stationary, moves sunward relative to them as shown in the figure. If GT stays on the sheath side of the center of the sequence, then the passage of the vortices is recorded as a clockwise rotation of the fluctuating flow component in the satellite frame. Since the plasma sheet-like ions are detected when the fluctuating flow is sunward and vice versa, the magnetopause surface is inferred to be deformed into the wavy pattern as shown in the figure. This suggests that the three hours of vortex activity at the MP was not enough to produce highly rolled-up vortices and direct transport of cold and dense magnetosheath plasma into the PS. Note that the PS adjacent to the MP stayed hot and tenuous at least until 2400 UT (cf. the two last panels of Figure 3).

[9] The origin of the vortices is unclear. The B_x component in the magnetosheath, that is the component parallel to the flow and presumably the wave number vector direction has a stabilization effect on the Kelvin-Helmholtz (KH) instability at the magnetopause, which would be the most popular mode that one tries to relate to vortices [*Miura*, 1995a, 1995b]. Indeed, the Alfvèn velocity computed using the sheath B_x component is calculated to be 175 km s^{-1}. This is close to if not more than half of the velocity difference across the magnetopause. Thus, it is questionable if the KH instability can have a significant growth rate to be responsible for the observed vortex sequence.

[10] At 0000 UT (11 January), increasing solar wind density pushed the MP further in and GT left the BL region. Until 0600 UT, except for a few brief excursions marked by positive V_x (2nd panel of Figure 3) into the PS, Geotail stayed mostly in the magnetosheath (Plasma data in the magnetosheath region are obtained by a different instrument mode and are not shown here). Figure 5 shows details of the brief PS excursion at 0430 UT. Shown are the V_x component, density, and the Et diagram of ions (omnidirectional). The flow is stagnant from 0425–0431:30 UT. There are two types of ion distribution detected during this interval. One is the nominal PS-like ion distribution, detected in the middle of the interval (0428–0430:30 UT). The PS distribution has a single energy peak at several keV. The second type of distribution is detected upon entry into and exit out of the stagnant region. This distribution exhibits mixing. One can clearly see in the Et diagram that the energy spectrum has two distinct peaks at <1 keV and several keV. The higher-energy component is quite similar to the PS component. The presence of a low-energy sheath-like component (<1 keV) simultaneous with the PS component implies that there was spatial mixing of the two components, but little mixing in velocity (energy) space. Ion mixing was not detected in the middle of the interval. Since the whole interval is ∼7 min, it is unlikely that GT penetrated deep into the PS. The shallow entry implies that mixed ions had not yet occupied a wide region of the PS adjacent to the MP at this time. That is, 7.5 hours after the northward turning at 2100 UT was not enough to produce a thick layer of the mixed ions.

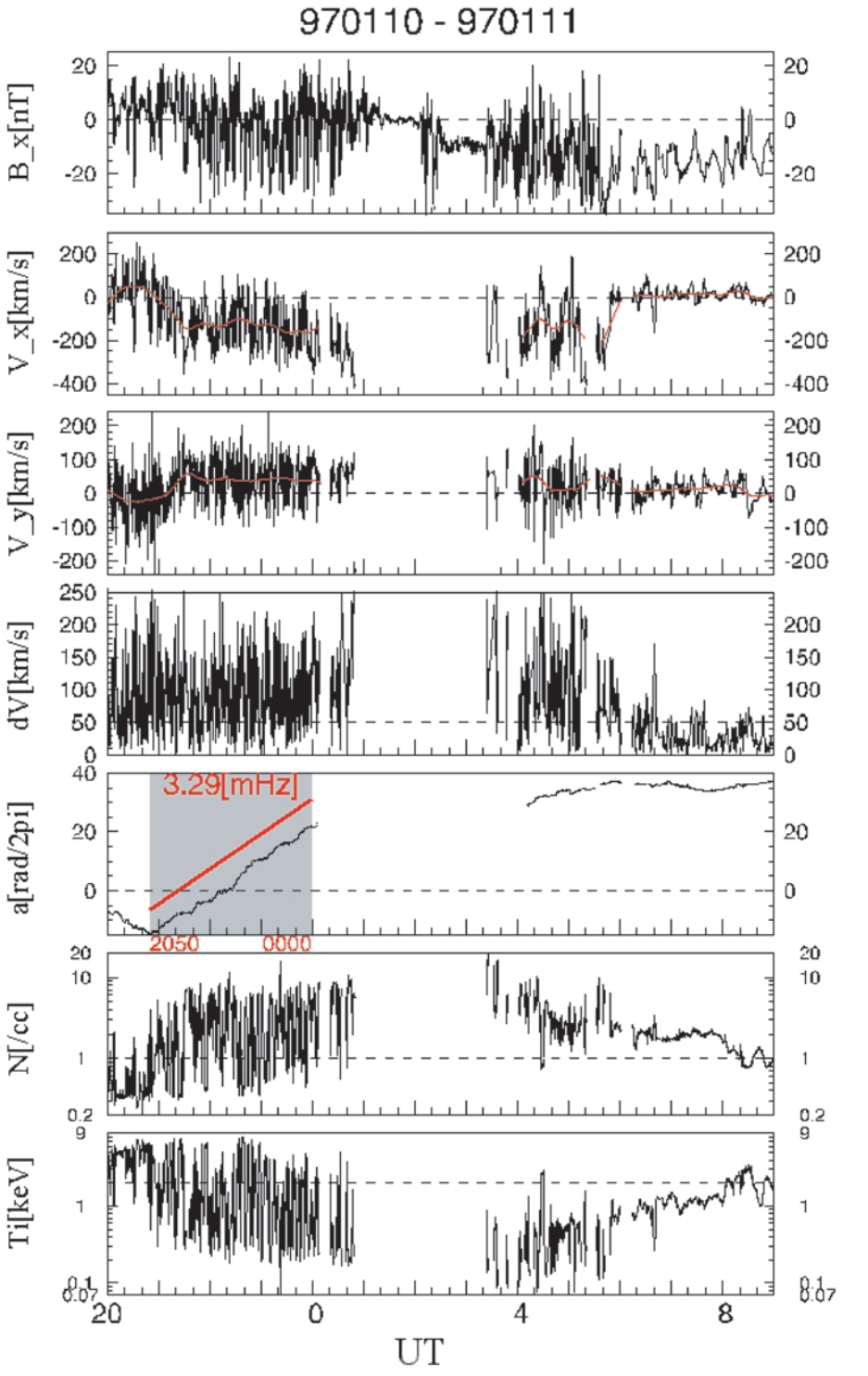

Figure 3. Geotail data for 10 January, 2000 UT, to 11 January, 0800 UT, taken in the duskside magnetotail. The time resolution is 12 s. Vortex-like activity in the boundary region at 2100–2400 UT, a brief entry into the PS from the sheath at 0430 UT and the cold-dense plasma sheet after 0600 UT are discussed.

[11] At 0600 UT, solar wind density decreased and Geotail reentered the PS at (X_{gsm}, Y_{gsm}) = (−14.5, 16.2) R_E. The PS at this time was cold and dense (6th and 7th panels of Figure 3, $T < 2$ keV, $n > 1$ cm^{-3}). The PS remained cold and dense as GT went deeper into the low-latitude PS ((−17.0 15.4) R_E at 0900 UT). In the Et diagram shown in Figure 6, one cannot recognize two distinct peaks in the count rate but the enhanced counts at lower energies are evident. This

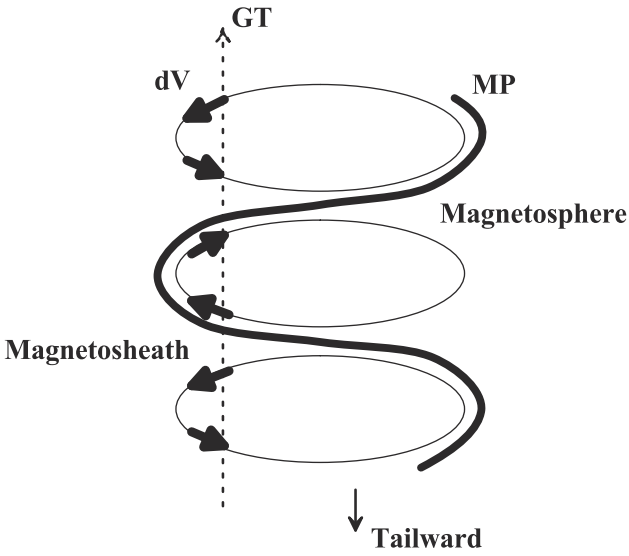

Figure 4. Schematic figure showing how the rotating feature of the fluctuating flow can be interpreted in terms of a sequence of vortices. The heavy line represents the magnetopause. We are looking down from the North.

lower-energy population is responsible for the cold-dense character [*Fujimoto et al.*, 1998]. This merging of hot PS with unheated sheath ions produces the cold-dense PS by 0600 UT, 9 hours after the northward turning of IMF. As previously reported [*Fujimoto et al.*, 1998], electrons in the 200–500 eV energy range (not shown) exhibit a bidirection anisotropy in this cold-dense part of the PS.

3.2. Interball-Tail Observations

[12] Figure 7 shows the Interball-Tail spacecraft (IT) data: The electron energy-time spectrogram from the ELECTRON experiment [*Sauvaud et al.*, 1997], the hydrogen energy-time spectrogram from the CORALL experiment [*Yermolaev et al.*, 1997], the B_x component of the magnetic field, the V_x and V_y components of the velocity, the density, and the ion temperature are shown. The time resolution is, respectively, 4 s for the magnetic field and 1 min for the plasma parameters. IT was in the duskside magnetotail, moving earthward from (X_{gsm}, Y_{gsm}) = (−15.8, 16.9) at 2100 UT (10 January) to (−10.8, 10.6) R_E at 0700 UT (11 January). Prior to 0100 UT, IT was in the PS, detecting hot-tenuous plasma. Until 0120 UT, when the jump in the solar wind density (0100 UT at Wind) caused IT to move into the magnetosheath, the low-latitude plasma sheet at the IT position (−14.2, 15.4) R_E remained hot and tenuous, despite the fact that GT observed vortex-like structures at the MP during this period. Furthermore, the PS remained hot-tenuous almost all the way to the MP, where there was a more or less rapid change to magnetosheath plasma. We conclude that a thick cold-dense layer adjacent to MP was developed neither at the GT ($X_{gsm} > -10$ R_E) nor at the IT ($X_{gsm} = -15$ R_E) positions by 0000 UT.

[13] The first drop in the solar wind density, from 0220–0320 UT, caused IT to return to the BL region. According to *Farrugia et al.* [2000], IT detected Kelvin-Helmholtz (KH) like waves. The frequency of these waves was 3.6 mHz, very close to the frequency observed at GT, suggesting that KH like waves continued from 2100 UT to 0320 UT (Note, however, that this wave activity is unlikely to be a KH instability in the interval from 2100 to 2400 UT for reasons discussed in the previous section). These waves, again, do not appear to be sufficient to bring magnetosheath plasma directly into the PS. After the second solar wind density drop at 0320 UT, IT observed the hot PS. This region was observed until 0530 UT.

[14] At 0530 UT, however, the ions started to show a mixing feature, which continued until 0630 UT. During this

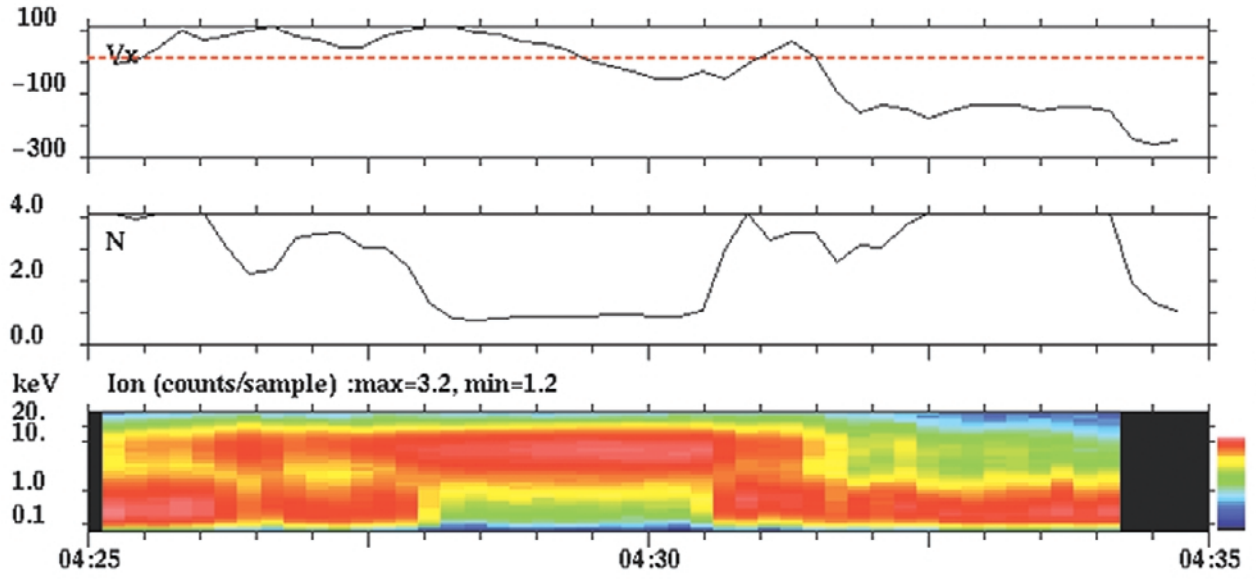

Figure 5. Expanded plot of the brief entry into the PS at 0430 UT. While ions do show mixing features upon entry into and exit out of the plasma sheet, ions in the middle of the interval are uncontaminated plasma sheet-like, suggesting mixing had not propagated deep into the plasma sheet.

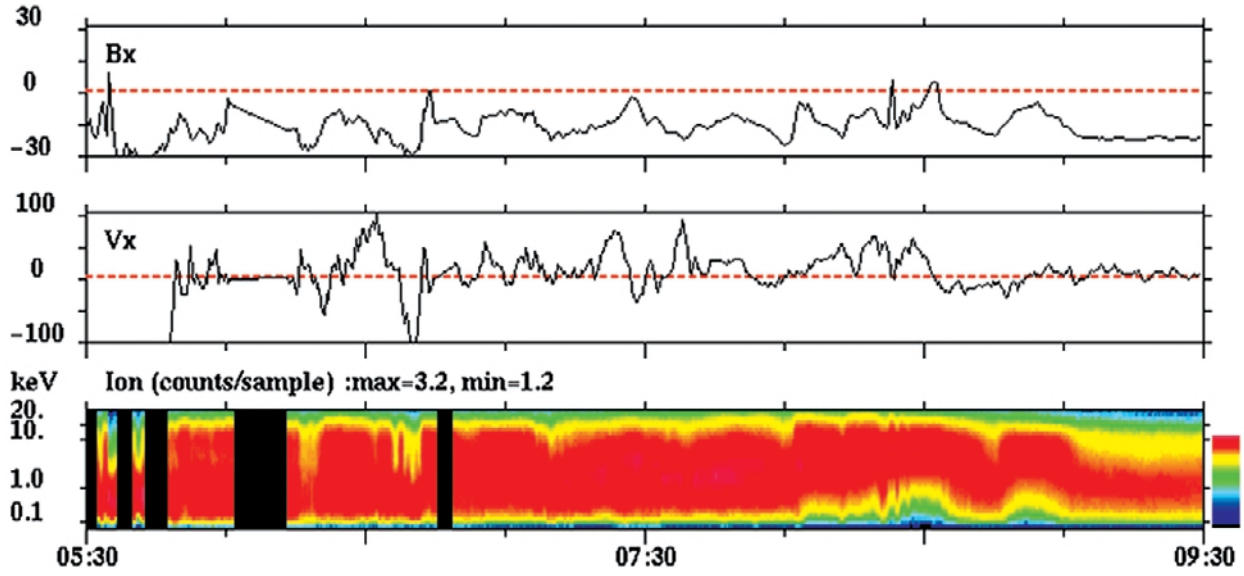

Figure 6. Ion Et diagram in the cold-dense plasma sheet obtained by the Geotail spacecraft. While a two-component feature is not evident, enhanced count rate at <1 keV range is responsible for the cold-dense status ($T < 2$ keV, $n > 1$ cm^{-3}). Comparison with Interball-Tail data confirms that thickening of the cold-dense part progressed in time.

interval, IT moved from (X_{gsm}, Y_{gsm}) = (−11.8, 12.2) to (−11.2, 11.1) R_E. This mixed region has density and temperature consistent with the cold-dense PS and is stagnant (see the V_x velocity in Figure 7). Electrons are found to show bidirectional anisotropy, details of which will be shown in a later section [e.g., *Fujimoto et al.*, 1998]. The entry of IT into this mixed region at 0530 UT is marked by a jump in $|B_x|$, indicating that this region is located at the high-latitude part of the PS. At 0630 UT, the satellite enters the lobe region, indicating that the mixed region was located at the highest-latitude part of the plasma sheet adjacent to the lobe region. GT was at the MP at 0600 UT at a more distant location ((X_{gsm}, Y_{gsm}) = (−14.5, 16.2) R_E). From this, one can tell that IT was more than 4 R_E deeper inside the magnetosphere.

3.3. Synthesis

[15] Putting GT and IT data together, vortex-like structures seem to have continued at the duskside MP for more than 6 hours, from 10 January, 2100 UT, to 11 January, 0330 UT. These structures do not appear to be responsible for direct transport of sheath plasma into the PS. The PS adjacent to MP was surveyed by GT at 0000 UT (X_{gsm} = −8.7 R_E) and by IT at 0100 UT (X_{gsm} = −14.2 R_E) and at 0330 UT (X_{gsm} = −13 R_E). Over this time period, neither spacecraft observed an extended region filled by mixed ions nor did they observe a cold-dense PS. In contrast, when IT shifted into a higher-latitude part of the PS at 0530 UT (X_{gsm} = −11.8 R_E) mixed ions appeared and stayed until IT went out into the lobe. Similarly, when GT reentered the PS at 0600 UT (X_{gsm} = −14.5 R_E) an extended cold-dense plasma sheet had already developed.

[16] One may argue for a temporal thickening of the cold-dense layer by comparing the IT data at 0000 UT and the GT data after 0600 UT. Both spacecraft were in the low-latitude plasma sheet at (X_{gsm}, Y_{gsm}) ∼ (−15, 16)R_E. At 0000 UT an earlier time, IT did not see cold-dense ions. At 0600 UT a later time, at the same location but deeper inside the PS, GT detected the cold-dense PS. Furthermore, the solar wind dynamic pressure was slightly lower during GT observations, suggesting GT was farther away from the MP. That is, the difference cannot be a spatial effect. There is also a hint from the GT data that a thick cold-dense layer had not yet developed by 0430 UT. The salient picture that comes out of these observations is that cold-dense layer seems to have thickened significantly between 0430 and 0530 UT. This is when the magnetosphere was expanding (so as to engulf the Geotail spacecraft at 0550 UT) in response to the decreased solar wind ram pressure. Some processes that were operative at the outward expanding MP under northward IMF is the agent for the plasma transport. Fortunately, the processes in the BL region were monitored by Interball-Aurora and Polar for this event and these observations will be described in the next section.

4. Low-Altitude Observations

4.1. DMSP Satellites' Observations

[17] It is not necessarily clear from the in situ observations whether the change in the plasma status detected at the spacecraft's position reflects a global change. On 11 January 1997, three DMSP satellites, F10, F12, and F13, were operational. They provide further evidence for the global plasma sheet cooling. The SSJ4 data from the 3 DMSP satellites are used to infer plasma sheet ion temperature (T), density (n), and pressure (p). The method has been fully described by *Wing and Newell* [1998; 2000]. The inferred plasma sheet temperature from each satellite pass was combined to create hourly temperature profile for the period from 10 January 1997, 2100 UT, to 11 January, 0800 UT. These hourly ion temperature profiles indicate that there are temperature fluctuations in the PS from 10 January, 2100

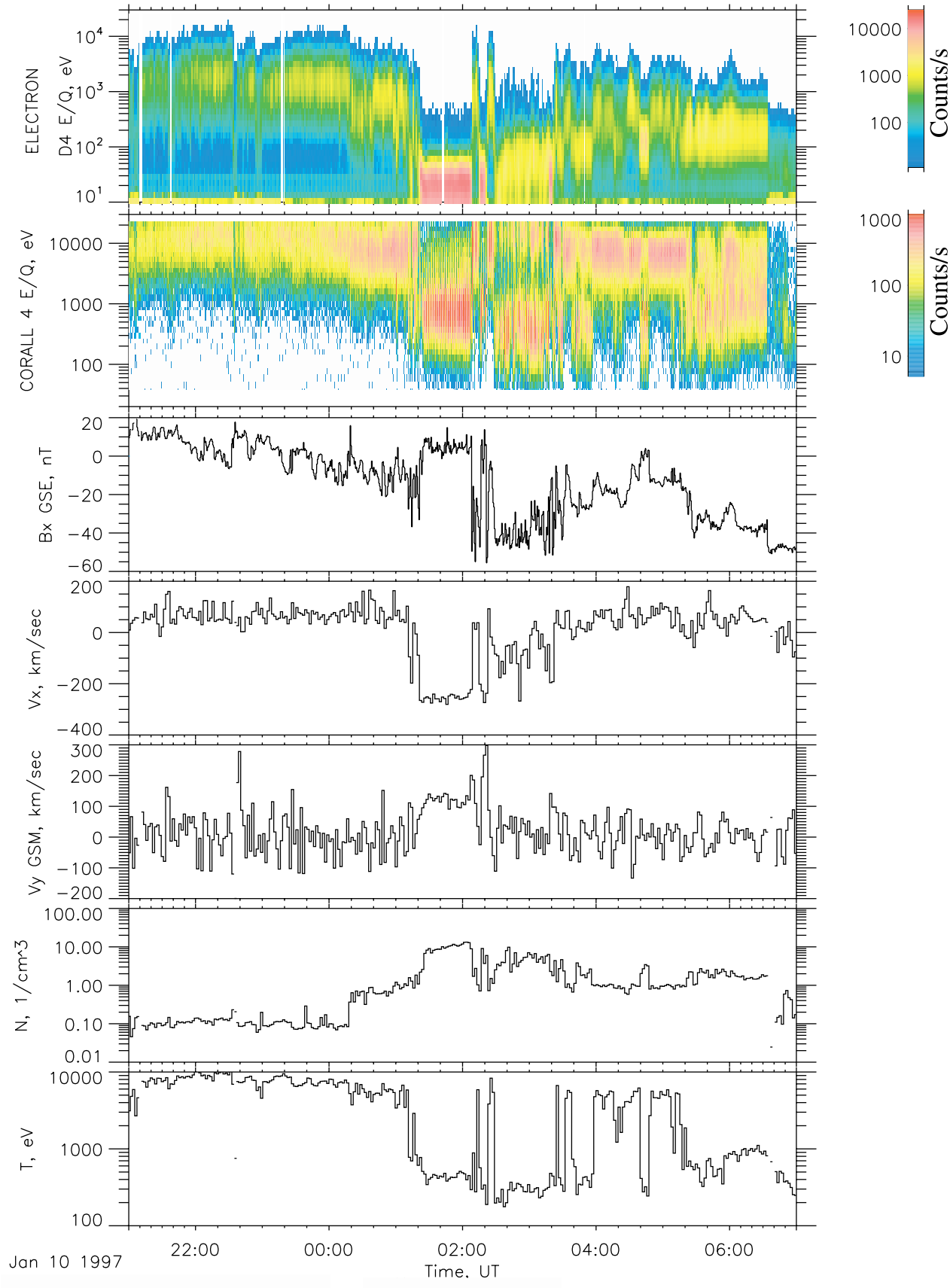

Figure 7. From top to bottom: electron and hydrogen Et diagram, B_x component (nT), V_x and V_y components (km s^{-1}), density (cm^{-3}), and temperature (eV) on January 10–11, 1997 between 2100 and 0700 UT measured by IT.

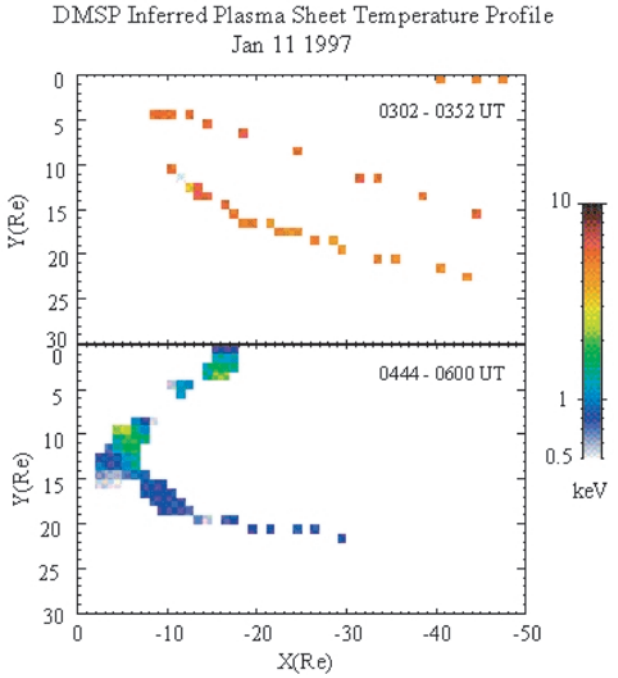

Figure 8. Temperature profiles obtained from the DMSP F10, F12, F13 data on 11 January 1997 between 0302 and 0352 UT, and between 0444 and 0600 UT. Profiles are calculated and projected in the equatorial plane using the method described by *Wing and Newell* [1998, 2000].

UT, to 11 January, 0800 UT. However, the most drastic temperature change by far occurred between the 0302–0352 UT and 0444–0600 UT profiles in Figure 8. This figure shows the temperature profiles projected in the equatorial plane. In the midnight-dusk sector, the plasma sheet temperature was >3 keV during the 0302–0352 UT interval but during the 0444–0600 UT interval the plasma sheet temperature was significantly cooler, <1.5 keV with the lowest temperature near the dusk flank. The observation suggests that there was a rather rapid cooling of the midnight-dusk sector of the magnetotail between ~0400 and 0500 UT. In any case, the observation indicates that certainly by 0600 UT the plasma in the midnight-dusk sector has cooled off. Simultaneously, the density increased during the same period (not shown). This set of observations is consistent with in situ high-altitude observations on GT and IT described in previous sections.

4.2. Interball-Auroral Observations

[18] Figure 9 presents the electron and hydrogen energy-time spectrograms and their corresponding pitch angles on 11 January 1997 between 0420 and 0610 UT measured by the ION experiment on board Interball-Auroral at 3 R_E altitude [see *Sauvaud et al.*, 1998, for more detail]. The MLT range is from ~16 h to ~23 h. According to the low-energy electrons, from 0520 to 0610 UT, IA is in a LLBL-like region [*Newell and Meng*, 1992]. From about 0420 to 0520 UT, the satellite passes through a transition region with plasma characteristic between the plasma sheet and LLBL, where the electron energy slowly decreases from plasma sheet-like (around 1 keV) to the LLBL-like (several hundred eV). The hydrogen spectrogram presents clear dispersed (or time-of-flight) structures, particularly between 0430 and 0540 UT. These structures are characterized by decreasing energy from about 10 keV down to several hundred eV and by weak pitch-angle modulation. The structures repeat and overlap. At 0435 UT, IA observes a clear dispersed O^+ structure (see Figure 9) and, during the whole period, O^+ ions up flowing from the ionosphere are detected. *Sandahl et al.* [1998] have already studied these structures with the PROMICS experiment onboard IA. They found that particles are injected from the dusk flank of the magnetosphere ~15–20 R_E tailward, near or just above the equatorial plane. *Stenuit et al.* [2001] have also studied many cases of similar dispersed structures at the dawnside and duskside of the auroral oval. They found that these events occur more frequently during northward IMF. Also, the dispersions are due to ion time-of-flight effects with injections from the flanks of the magnetosphere. Here, we use the same method as *Stenuit et al.* [2001] to determine the approximate location of the particles sources. The trajectories of the particles forming the core of the dispersion (pixels in the Et diagram showing the maximum flux) have been propagated backward in time using a single particle trajectory code and the Tsyganenko 1996 magnetic field model [*Tsyganenko*, 1995; *Tsyganenko and Stern*, 1996]. Figure 10 presents results of this modeling for the energy dispersed structure observed in the LLBL projection at ~0512 UT (Plate 6). Each line represents a particle from the injection beginning at 0512 UT. Figure 10 displays the energy evolution, the pitch angles, the magnetic local times, the distances from Earth, and, the SM latitudes of selected particles. We find a focal point that corresponds to the approximate location of the source of the particles. Particles were injected nearly simultaneously, around (MLT, distance from Earth, magnetic latitude) ~ (21.5 h, 20 R_E, 35°), which correspond to (X_{gsm}, Y_{gsm}, Z_{gsm}) ~ (−17, 10, 5)R_E. This region is situated near the equatorial plane, near the dusk magnetopause, and is not so far from the location of GT and IT. Comparison of IA and IT data will be discussed in section 5.

4.3. Polar Observations

[19] The electron, hydrogen, and oxygen Et diagrams on 11 January 1997 between 0400 and 0700 UT obtained by the TIMAS instrument on board the Polar spacecraft are display in Figure 11. During the time interval, the altitude of the satellite remained near 6 R_E and in an MLT range is from ~17 h to ~ 21 h. The Polar TIMAS instrument obtains a mass spectrum every 3 min from 6 different look angles and 8 different energies. Using these data and the magnetic field direction, we obtained the mass spectrum at a given energy looking parallel and antiparallel to the magnetic field.

[20] Starting at 0400 UT until 0420 UT, the spacecraft is in the plasma sheet. There are reasonably high fluxes of 10 keV protons, almost no He^{2+} (not shown), and some substantial O^+. From around 0420 UT to around 0620 UT, there are repetitive dispersed ion signatures that overlap each other, similar to those observed by IA. We have computed the distance to the source region by the method described by *Fuselier et al.* [2000]. It is based on the cut off velocities of the down going and the return ion beam. The distance to the injection obtained by this method is about 15 R_E, that is, on the flank of the magnetosphere at about the

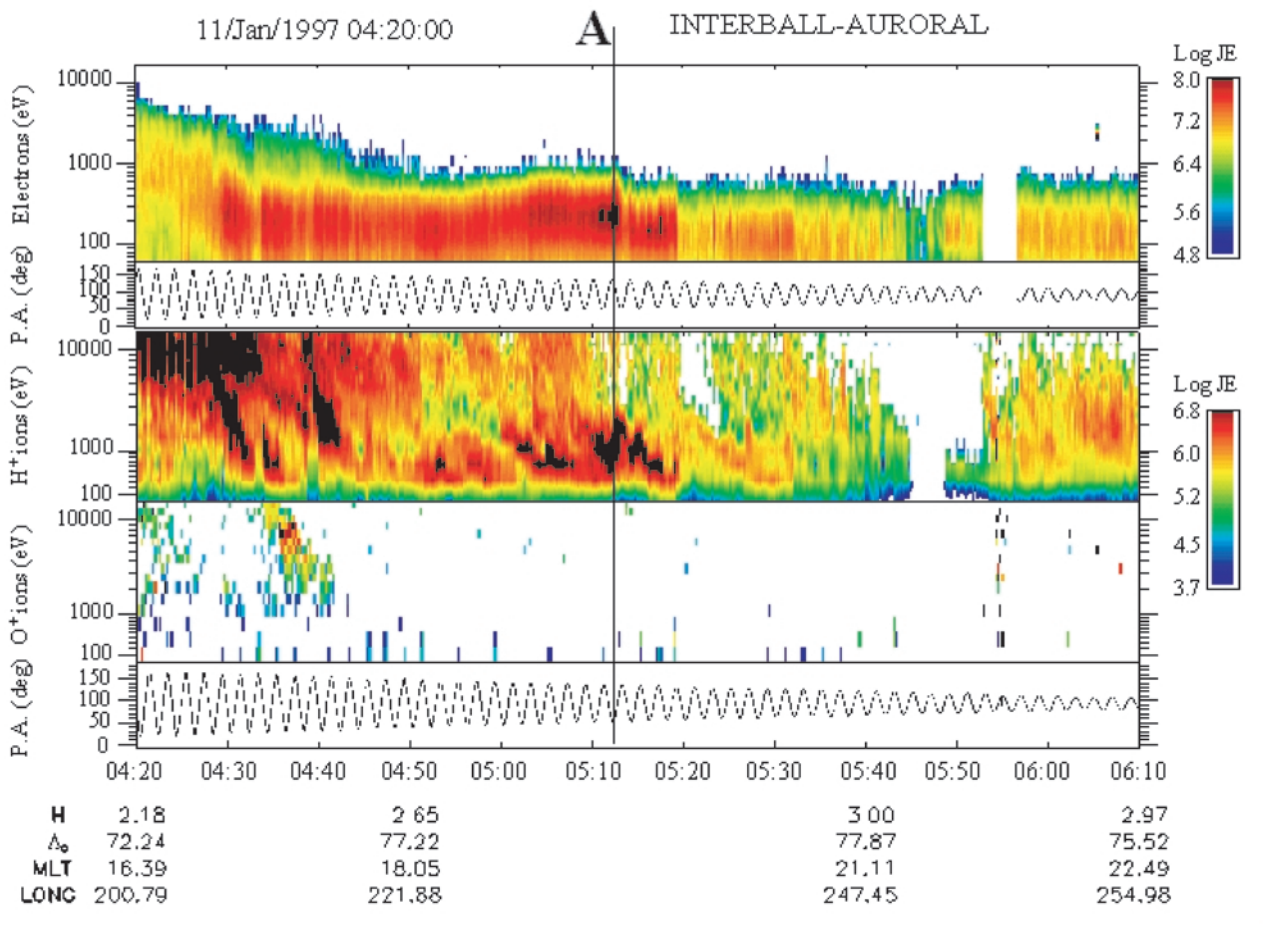

Figure 9. Electron, hydrogen and oxygen Et diagram and their corresponding pitch angles on 11 January 1997 between 0420 and 0610 UT obtained IA (see text).

same as for IA observations. The difference between the two observations is that the dispersions seen by Polar seem to show a more or less periodic feature, with a period of around 5 min.

[21] In this region, the energetic electron flux (E > 1 keV) is very low, possibly suggesting either that the magnetic field lines were at least open at one time (so that the energetic electrons from the magnetosphere had time to leave) or that this region, can not be reached by drifting plasma sheet electrons. However, two types of mass spectra are seen. The main difference is the flux level of the He^{2+}. In the first mass spectrum (Figure 12a), the He^{2+} flux is ~1% of the H^+ flux, in the second one, (Figure 12b), it is ~2%. In both spectra, there is counter streaming O^+. At 1.72 keV/e, the O^+ flux is balanced between parallel and antiparallel fluxes. This indicates that the field line is closed, allowing O^+ from both hemispheres (or from one hemisphere and a mirror point in the opposite hemisphere) to arrive at the spacecraft. Note that in Figure 12b, the O^+ flux is counter streaming, although the flux parallel to the magnetic field (toward the ionosphere) is higher than that antiparallel to the magnetic field. The differences between the parallel and antiparallel fluxes are the result of velocity dispersion signatures observed throughout the period from 0420 to about 0550 UT (higher velocity O^+ traveling a greater distance arrives at the same time as lower velocity O^+ traveling a lesser distance). This closed magnetic field topology persists for sometime. In fact, the same dispersed structures that are seen in the protons (and the He^{2+}) are seen in the O^+. Sometimes, there is a very clear energy separation between the O^+ populations. Thus, for example, at 0548 UT, (not shown) the O^+ population at several hundred eV is propagating only away from the ionosphere (antiparallel to the magnetic field direction) but the population above 1 keV/e is propagating mainly toward the ionosphere (parallel to the magnetic field direction).

[22] At 0550 UT, the characteristics of the O^+ population change considerably. At this time, there is no longer any population propagating parallel to the magnetic field. In other words, there is only ion outflow (even though there is still considerable He^{2+} and H^+ present). This region looks just like the mantle. There is a cold, flowing O^+ outflow population mixed with a solar wind population that is propagating mainly antiparallel to the magnetic field (i.e., these are the ions that bounce at low altitudes and return along open field lines toward the tail).

4.4. Synthesis

[23] Between 0400 and 0600 UT, Polar and IA were both at low altitude, at MLT = 17–21, detected high fluxes of low-energy electrons and ions, with ions showing energy dispersed structures. From the electron and the mass spec-

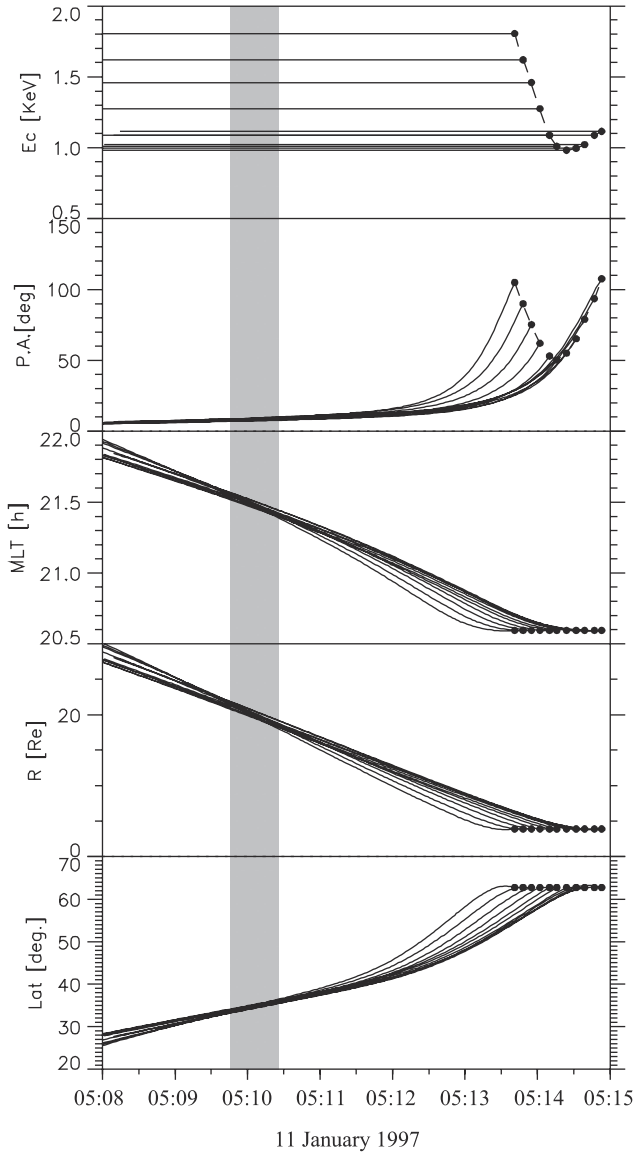

Figure 10. Details of the backward trajectory computations for the injection beginning at 0512 UT on 11 January 1997 (noted A in Figure 9). The trajectories of particles (coded with different colors lines) are computed backward in time from the shape of the energy/pitch angle time of flight dispersed structures. The *Tsyganenko* [1995] magnetic field model is used for 3D computations. From top to bottom: Evolution of the energies and the pitch angles, calculated MLT (hours), distance from Earth (Earth radii), and magnetic latitude (degrees) of selected particles.

trum data obtained on board Polar, we infer the nature of the field lines that crossed the satellite. The field lines observed by Polar from about 0420 to 0550 UT were possibly open at one time (causing the loss of energetic electrons) but were closed prior to the observations by the Polar spacecraft (resulting in the counter streaming O^+). From 0550 UT, the spacecraft was on the field lines that seem to be open (from the lack of counter streaming O^+). These field lines look very much like the mantle observed at high latitudes for southward IMF. From the Polar and IA data, the possible source of the dispersed injections is located near the equatorial plane and near the MP in the dusk flank of the magnetosphere, 15 R_E down the tail.

5. Discussion and Conclusion

[24] During the northward IMF interval for 10–11 January 1997 magnetic cloud event, seven satellites were located in the key regions of the magnetosphere. This configuration allows us to study the dynamics of the dusk-flank magnetopause and its possible role in the local transport of magnetosheath plasma into the magnetosphere. In the previous sections, we have discussed independently the high- and low-altitude observations. We noted that the possible source location for the energy-dispersed ions observed at low altitude by Polar and IA is the dusk flank of the magnetosphere. The GT and IT spacecraft, located at the dusk-flank magnetopause, detected cold-dense plasma. Here we show the connectivity among spacecraft in a more direct manner. During the injections (between 0420 and 0550 UT), the highest and the lowest pitch angles observed by IA are, respectively, around 135° and 45°. Assuming that IA and IT are on the same magnetic field line, pitch angles of 135° and 45° on IA at low altitudes correspond to pitch angles of 9° on IT at high altitudes. Fluxes of field-aligned electrons parallel and antiparallel to the magnetic field at IT should be balanced if the field lines are closed and the characteristics of the energy spectrum should be the same as those of 45°/135° electrons at IA. Figure 13 represents the energy-flux spectra for parallel and antiparallel electrons measured by IT in the mixed ion region (between 0530 and 0630 UT), and for 45°/135° electrons measured by IA in the dispersed-ion interval (between 0440 and 0520 UT). Spectra are taken when each satellite was located at $X_{\mathrm{gsm}} \sim -25$ R_E (projection for IA along the field line of the Tsyganenko 1996 model) and separated along the Y axis by less than 2 R_E. Both are just inside the model magnetosphere, close to the magnetopause. Figure 13 shows that electrons observed by IA and IT during these periods have essentially the same characteristics and that the fluxes parallel and antiparallel to the magnetic field are well balanced. The bidirectional electrons suggest the closed topology of the field lines. Furthermore, they confirm that the field lines corresponding to mixed ions in the plasma sheet have their root in the dusk-auroral oval where dispersed ions are observed. The mixed ions do not show any distinct features when observed locally by high-altitude spacecraft (at the MP), but, when viewed globally, are embedded in a region where a process leading to dispersed-ion precipitation is operative.

[25] The change from hot-tenuous to cold-dense plasma sheet seems to have taken place rather quickly starting at ~0500 UT. Concurrent with this change at the MP two low-altitude spacecraft were detecting injections of magnetosheath-like ions in the dusk-auroral oval. A time-of-flight analysis showed that the ions originate from the tail-flank at some 15 R_E down the tail. There are two ways to interpret these observations: One way is to interpret the "injection" as merely precipitation of ions that had somehow entered the magnetosphere. That is, injection has no close relevance to the transport across the magnetopause. Even in this case, the Polar data show that the boundary layer region must have been perturbed quasiperiodically to produce the qua-

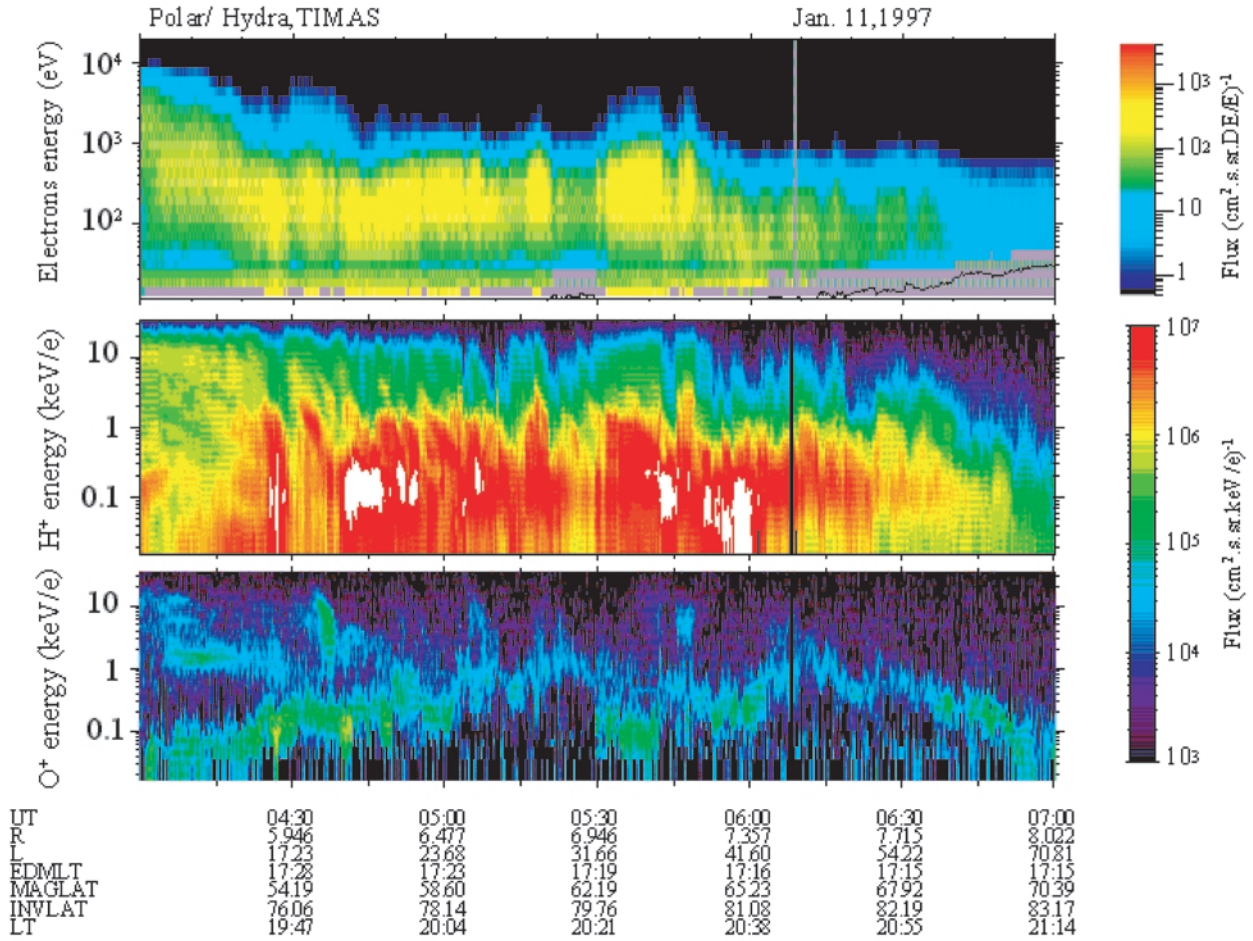

Figure 11. Electron, hydrogen and oxygen Et diagram on 11 January 1997 between 0400 and 0700 UT obtained by Polar.

siperiodic precipitation pattern in the Et diagram. The other way is to interpret the ''injection'' feature as evidence for real injection of magnetosheath ions on to the magnetospheric field lines.

[26] The solar wind/IMF condition around the time of the change in the character of the plasma sheet is important for the interpretation of the injection feature. By taking the time lag from the Wind spacecraft to the magnetopause into account, the sequence of events are as follows: the IMF turned northward at 2100 UT and became strongly northward ($B_z > |B_y|$) at 0200 UT in the midst of the high solar wind density interval. The solar wind density and dynamic pressure were anomalously high until 0220 UT. They were still high until 0320 UT, when they became more nominal. If we take the time of the plasma sheet status transition to be at 0500 UT, then this is 8 hours after the northward IMF turning, 3 hours after the IMF became strongly northward (including the anomalously high solar wind density interval), and 1.5 hours after the return to nominal solar wind condition (density, dynamic pressure) with a strong northward IMF. Note that it is likely that the magnetosphere was gradually expanding in this 1.5-hour interval.

[27] A Kelvin-Helmholtz wave driven by the velocity shear at the magnetopause has been proposed as a possible mechanism of the magnetosheath plasma entry [*Fujimoto and Terasawa*, 1994; *Fairfield et al.*, 2000; *Otto and Fairfield.*, 2000; *Nykyri and Otto*, 2001]. Vortex-like feature at the magnetopause were detected more than 6 hours prior to the time of the change in the PS and the period of the vortex-like wave is similar to the period of injections observed by Polar. However, the vortices detected by Geotail are not necessarily evidence of the KH instability. Also, this wave does not appear to transport plasma across the MP. The cold-dense layer remained thin despite the fact that vortex-like activity existed for more than 6 hours. Indeed the cold-dense layer appears to have grown rather quickly around 0500 UT. The characteristic time scale of hours is much longer than the dynamical time scale for vortices. One possible explanation is that the boundary condition for the vortices, be it of KH origin or not, did not allow them to develop into a nonlinear stage until 0500 UT. At that point, highly rolled-up vortices were formed, causing massive transport.

[28] *Stenuit et al.* [2001] report a case in which ion injections similar to the present case had a good correlation with pressure variation in the adjacent magnetosheath. Inspecting the solar wind data around 0500 UT (Figure 2), we note that there are variations in the dynamic pressure that could have caused the injections. In addition to the origin in the solar wind, the pressure variation can be generated at the bow shock or at the magnetopause boundary. Quasiperiodicity seen in the Polar data prefers a

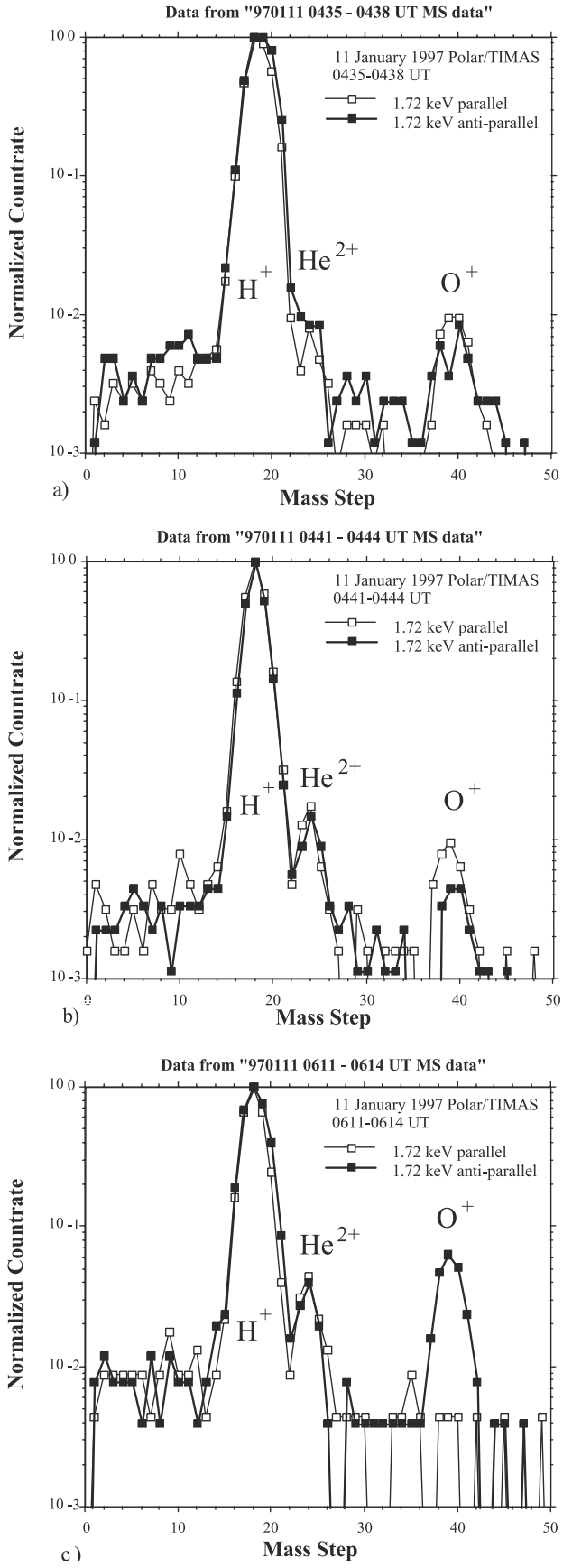

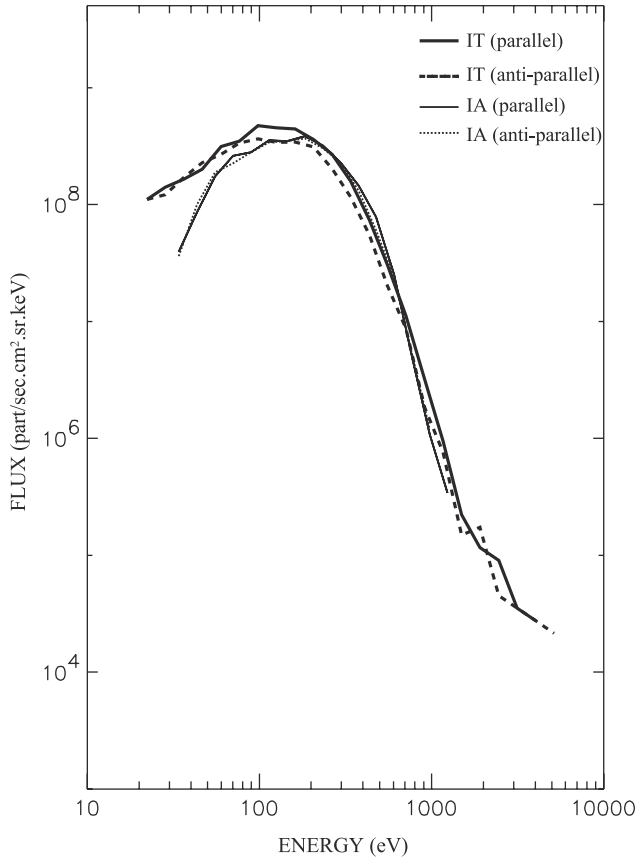

Figure 13. Electron energy flux spectra measured by IT and IA in parallel and antiparallel directions (see text).

magnetopause surface wave as the origin of the pressure disturbance. A puzzle here is the fact that massive transport did not occur before 0500 UT despite significant dynamic pressure variations. Also, the reason why the high solar wind density interval was not preferred is puzzling.

[29] Reduced flux of energetic electrons seen by IA and Polar may suggest that the field lines were once opened. The injection might be related to reconnection that is closing the field lines that experienced reconnection on the dayside and then convected tailward. The time-of-flight analysis indicates that the reconnection is taking place at some X = −15 R_E. The quasiperiodicity in the Polar data may show that the reconnection is regulated by a surface wave activity. In this interpretation, the overlapping in time of neighboring ion dispersion events would imply that the field line that was once open will experience another reconnection with a different open field line within relatively short interval.

Figure 12. (opposite) a) Mass spectrum from the TIMAS instrument at 0435–0438 UT. The major mass peaks are labeled from their positions computed from instrument calibration data. At 1.72 keV/e, the O^+ flux is balanced between parallel and antiparallel fluxes. b) Mass spectrum at 0441–0444 UT. Again, the O^+ is counter streaming. c) Mass spectrum from the "mantle" region after 0550 UT. Note that there is significant H^+ and He^{2+} present but that the O^+ is propagating entirely antiparallel to the magnetic field (away from the ionosphere) (see text).

[30] In conclusion, we have reported observations of ion injections in the dusk oval when the plasma sheet status was changing to cold-dense. The injections suggest a dynamical situation of the magnetopause-boundary layer region when the cold-dense plasma sheet was forming. The physical mechanism of this formation still needs to be studied. In particular, northward turning does not instantaneously lead to the status change even in the plasma sheet adjacent to the magnetopause. Furthermore, there could be a long delay in the formation of the cold-dense PS, depending on external conditions that are not known at present. Our hope is that this multipoint study will stimulate further study using low-altitude satellite data on the entry of magnetosheath plasma across the flanks during strong northward IMF periods.

[31] **Acknowledgments.** We thank K. W. Ogilvie and R. P. Lepping for providing the MFI and 3DP Wind data. M. F. thanks T. Tonooka for his help in Geotail data analyses. The study was initiated at the ISSI workshop on "Multi-scale dynamic processes in the magnetospheric boundary layers and the cusp". Research at CESR was supported by a CNES contract. Research at Lockheed Martin was conducted under the Polar-Interball Guest investigation subcontract 999095Q. S. Wing would like to acknowledge the support of NASA grants NAG5-10971 and NAGW-19512.

[32] Lou-Chuang Lee and Chin S. Lin thank Toshio Terasawa and another reviewer for their assistance in evaluating this paper.

References

Fairfield, D. H., A. Otto, T. Mukai, S. Kokubun, R. P. Lepping, J. T. Steinberg, A. J. Lazarus, and T. Yamamoto, Geotail observations of the Kelvin-Helmholtz instability at the equatorial magnetotail boundary for parallel northward fields, *J. Geophys. Res.*, *105*, 21,159, 2000.

Farrugia, C. J., et al., Coordinated Wind, Interball/tail, and ground observations of Kelvin-Helmholtz waves at the near-tail, equatorial magnetopause at dusk, January 11, 1997, *J. Geophys. Res.*, *105*, 7639, 2000.

Fujimoto, M., and T. Terasawa, Anomalous ion mixing within an MHD scale Kelvin-Helmholtz vortex, *J. Geophys. Res.*, *99*, 8601, 1994.

Fujimoto, M., T. Terasawa, T. Mukai, Y. Saito, T. Yamamoto, and S. Kokubun, Plasma entry from the flanks of the near-Earth magnetotail: Geotail observations, *J. Geophys. Res.*, *103*, 4391, 1998.

Fujimoto, M., T. Mukai, A. Matsuoka, Y. Saito, H. Hayakawa, S. Kokubun, and R. P. Lepping, Multi-point observations of cold-dense plasma sheet and its relation with tail-LLBL, *Adv. Space. Res.*, *25*(7/8), 1607, 2000.

Fuselier, S. A., R. C. Elphic, and J. T. Gosling, Composition measurements in the dusk flank magnetosphere, *J. Geophys. Res.*, *104*, 4515, 1999.

Fuselier, S. A., S. M. Petrinec, and K. J. Trattner, Stability of the high-latitude reconnection site for steady northward IMF, *Geophys. Res. Lett.*, *27*, 473, 2000.

Le, G., C. T. Russell, J. T. Gosling, and M. F. Thomsen, ISEE observations of low-latitude boundary layer for northward interplanetary magnetic field: Implications for cusp reconnection, *J. Geophys. Res.*, *101*, 27,239, 1996.

Lennartsson, W., A scenario for solar wind penetration of Earth's magnetotail based on ion composition data from the ISEE 1 spacecraft, *J. Geophys. Res.*, *97*, 19,221, 1992.

Lepping, R. P., et al., The Wind magnetic field investigation, *Space Sci. Rev.*, *71*, 207, 1995.

Mitchell, D. G., F. Futchko, D. J. Williams, T. E. Eastman, L. A. Frank, and C. T. Russell, An extended study of the low latitude boundary layer on the dawn and dusk flanks of the magnetosphere, *J. Geophys. Res.*, *92*, 7394, 1987.

Miura, A., Kelvin-Helmholtz instability at the magnetopause: Computer simulations, in *Physics of the Magnetopause*, *Geophys. Monogr. Ser.*, vol. 90, p. 285, AGU, Washington, D.C., 1995a.

Miura, A., Dependence of the magnetopause Kelvin-Helmholtz instability on the orientation of the magnetosheath magnetic field, *Geophys. Res. Lett.*, *22*, 2993, 1995b.

Newell, P. T., and C.-I. Meng, Mapping the dayside ionosphere to the magnetosphere according to particle precipitation characteristics, *Geophys. Res. Lett.*, *19*, 609, 1992.

Nishikawa, K.-I., Particle entry through reconnection grooves in the magnetopause with a dawnward IMF as simulated by a 3-D EM particle code, *Geophys. Res. Lett*, *25*, 1609, 1998.

Nykyri, K., and A. Otto, Plasma transport at the magnetospheric boundary due to reconnection in Kelvin-Helmholtz vortices, *Geophys. Res. Lett*, *28*, 3565, 2001.

Ogilvie, K. W., et al., SWE: A comprehensive plasma instrument for the Wind spacecraft, *Space Sci. Rev.*, *71*, 55, 1995.

Otto, A., and D. H. Fairfield, Kelvin-Helmholtz instability at the magnetotail boundary: MHD simulation and comparison with Geotail observations, *J. Geophys. Res.*, *105*, 21,175, 2000.

Phan, T. D., R. P. Lin, S. A. Fuselier, and M. Fujimoto, Wind observations of mixed magnetosheath-plasma sheet ions deep inside the magnetosphere, *J. Geophys. Res.*, *105*, 5497, 2000.

Raeder, J., J. Berchem, M. Ashour-Abdalla, L. A. Frank, W. R. Paterson, K. L. Ackerson, S. Kokubun, T. Yamamoto, and J. A. Slavin, Boundary layer formation in the magnetotail: Geotail observations and comparisons with a global MHD simulation, *Geophys. Res. Lett.*, *24*, 951, 1997.

Sandahl, I., H. E. J. Koskinen, A. M. Mälkki, T. I. Pulkkinen, E. Y. Budnik, A. O. Fedorov, L. A. Frank, and J. B. Sigwarth, Dispersive magnetosheath-like ion injections in the evening sector on January 11, 1997, *Geophys. Res. Lett.*, *25*, 2568, 1998.

Sauvaud, J.-A., P. Koperski, T. Beutier, H. Barthe, C. Aoustin, J. J. Thocaven, J. Rouzaud, E. Penou, O. Vaisberg, and N. Borodkova, The Interball-Tail ELECTRON experiment: Initial results on the low-latitude boundary layer of the dawn magnetosphere, *Ann. Geophys.*, *15*, 587, 1997.

Sauvaud, J. A., H. Barthe, C. Aoustin, J. J. Thocaven, J. Rouzaud, E. Penou, D. Popescu, R. A. Kovrazhkin, and K. G. Afanasiev, The ION experiment onboard the Interball-Auroral satellite: Initial results on velocity-dispersed structures in the cleft and inside the auroral oval, *Ann. Geophys.*, *16*, 1056, 1998.

Shue, J. H., et al., Magnetopause location under extreme solar wind conditions, *J. Geophys. Res.*, *103*, 17,691, 1998.

Song, P., T. I. Gombosi, D. L. Dezeeuw, K. G. Powell, and C. P. T. Groth, A model of solar wind-magnetosphere-ionosphere coupling for due northward IMF, *Planet. Space Sci.*, *48*, 29, 2000.

Stenuit, H., J.-A. Sauvaud, D. C. Delcourt, T. Mukai, S. Kokubun, M. Fujimoto, N. Y. Buzulukova, R. A. Kovrazhkin, R. P. Lin, and R. P. Lepping, A study of ion injections at the dawn and dusk polar edges of the auroral oval, *J. Geophys. Res*, *106*, 29,619, 2001.

Terasawa, T., et al., Solar wind control of density and temperature in the near-Earth plasma sheet: Wind/Geotail collaboration, *Geophys. Res. Lett.*, *24*, 935, 1997.

Tsyganenko, N. A., Modeling the Earth's magnetospheric magnetic field confined within a realistic magnetopause, *J. Geophys. Res.*, *100*, 5599, 1995.

Tsyganenko, N. A., and D. P. Stern, Modeling the global magnetic field of the large-scale Birkeland current systems, *J. Geophys. Res.*, *101*, 27, 187, 1996.

White, W. W., G. L. Siscoe, G. M. Erickson, Z. Kaymaz, N. C. Maynard, K. D. Siebert, B. U. Ö. Sonnerup, and D. R. Weimer, The magnetospheric sash and the cross-tail S, *Geophys. Res. Lett*, *25*, 1605, 1998.

Wing, S., and P. T. Newell, Central plasma sheet ion properties as inferred from ionospheric observations, *J. Geophys. Res.*, *103*, 6785, 1998.

Wing, S., and P. T. Newell, Quiet time plasma sheet ion pressure contribution to Birkeland currents, *J. Geophys. Res.*, *105*, 7793, 2000.

Yermolaev, Y. I., et al., Ion distribution dynamics near the Earth's bow shock: First measurements with the 2D ion energy spectrometer CORALL on the INTERBALL/Tail satellite, *Ann. Geophys.*, *15*, 533, 1997.

V. Angelopoulos, J. Bonnell, and T. D. Phan, Space Sciences Laboratory, Berkeley, CA 94720, USA.

E. Budnik, A. Fedorov, J.-A. Sauvaud, and H. Stenuit, CESR/CNRS, 9 avenue du Colonel Roche, BP 4346, 31028 Toulouse cedex 4, France. (helene.stenuit@cesr.fr)

M. Fujimoto, Department of Earth and Planetary Science, TITECH, Okayama, Meguro 152, Tokyo, Japan.

S. A. Fuselier, and K. J. Trattner, Lockheed Martin Palo Alto Laboratory, 3251 Hanover Street, Palo Alto, CA 94304-1191, USA.

T. Mukai, ISAS, 3-1-1 Yoshinodai, Sagamihara, Kanagawa 229-8510, Japan.

A. Pedersen, Department of Physics, Oslo University, P. O. Box 1048 Blindern, N-0316 Oslo, Norway.

S. P. Savin, Space Research Institute, Academy of Sciences, Profsyuznaya 84/32, 117810 Moscow, Russia.

S. Wing, Applied Physics Laboratory, Johns Hopkins University, 11100 Johns Hopkins Road, MD 20723-6099, USA.